Aluminum Equation-of-State Data in the Warm Dense Matter Regime

P. Renaudin,* C. Blancard, J. Clérouin, G. Faussurier, P. Noiret, and V. Recoules

Département de Physique Théorique et Appliquée, CEA/DAM Ile-de-France, BP12, F-91680 Bruyères-le-Châtel Cedex, France

(Received 25 November 2002; published 12 August 2003)

Isochore measurements were performed in the warm dense matter regime. Pressure and internal energy variation of aluminum plasma (density 0.1 g/cm^3 and 0.3 g/cm^3) are measured using a homogeneous and thermally equilibrated media produced inside an isochoric plasma closed vessel in the internal energy range 20–50 MJ/kg. These data are compared to detailed calculations obtained from *ab initio* quantum molecular dynamics, average atom model within the framework of the density functional theory, and standard theories. A dispersion between theoretical isochore equation of state is found in the studied experimental thermodynamic regime.

DOI: 10.1103/PhysRevLett.91.075002 PACS numbers: 52.25.–b, 52.25.Kn, 52.27.Gr

The equation of state (EOS) of most materials is fairly well known under many conditions. In warm dense matter, which defines a part of the density-temperature plane between a solid and plasma, the description of physics is complicated due to the strong interaction between particles. This thermodynamic regime is typically encountered in planetary interiors, cool dense stars, and in inertial confinement implosion. In this domain, standard theories of condensed matter and/or plasma statistical physics are questionable [1]. Knowledge of the EOS of such strongly coupled plasmas (SCP's), characterized by the Coulomb potential energy between plasma particles greater than their average kinetic energy, is therefore a crucial point. Many theories have been used to produce EOS tables, among which the SESAME tables [2] are the most commonly used. However, there are almost no available experimental data which can validate these calculations in this particular regime [3].

In this Letter, we report on the pressure and internal energy variation measurements of well-known mass density aluminum plasma. Our data allow therefore the first direct comparison of isochore measurements of aluminum SCP's with theoretical calculations. These results give access to the caloric properties of matter, i.e., the dependence of internal energy with respect to pressure and volume. Knowledge of the temperature or entropy is required to complete the thermodynamic equations and obtain quantities, such as heat capacity or sound velocity.

The experiments were performed inside an isochoric plasma closed vessel (EPI for Enceinte à Plasma Isochore), where a 25-μm-thick pure aluminum foil is heated by a slow (400 μs) electrical discharge and goes from the solid state at normal density and room temperature to a well-defined average density plasma. The details of the experimental setup used in these experiments are similar with the ones described in Ref. [4]. The plasma volume is controlled mechanically by the closed-vessel sapphire walls. The characteristic time of the electrical discharge is long enough to allow for the formation of a homogeneous plasma, and is short enough to limit the effects of the wall ablation.

Since the plasma is homogeneous, its average density is obtained by dividing the initial mass of the material placed inside the vessel by the volume of the vessel (22 cm^3). A Rogowski belt surrounds one electrode to measure the time derivative of the current and a resistive divider is used to measure the voltage drop across the plasma. Two piezoelectrical sensors with 2 μs rise time are placed at each end of the sapphire tube to measure the pressure during the discharge. The sensors are acceleration compensated and allow one to measure a maximum pressure (0.7 GPa) lower than the plasma pressure. There is no contact between them and the plasma. A surface divider piston reduces by a factor of 4 the applied pressure and transmits it to the sensor. A dynamic and static calibratation is performed before each experiment. A free-falling known mass is dropped onto a piston, creating a pressure pulse onto the sensor. By measuring the drop-mass velocity before and after the impact, the applied momentum on the sensor is deduced. The uncertainty in the drop-mass after impact velocity measurements produces a 15% uncertainty in the pressure of the plasma. To measure the static coefficient, a well-defined force is applied to the sensor. The force is obtained by measuring the crushing of small copper cylinders. These two procedures lead to two different calibration coefficients which are equal to within 5%.

In one electrical discharge, the experimental setup allows simultaneous measurements of internal energy variation ΔU_{int} and pressure P along an isochore. A schematic representation of the thermodynamic path (TP) in the vessel is shown in Fig. 1. Figure 2 shows the measured pressure as a function of the measured internal energy variation in the case of aluminum (nominal density 0.1 g/cm^3). The heating of the sample is assumed to be already isochoric when the vapor ionization induces an arc regime, at time t_0. The plasma is heated during more than 200 μs and reached the maxima of electrical

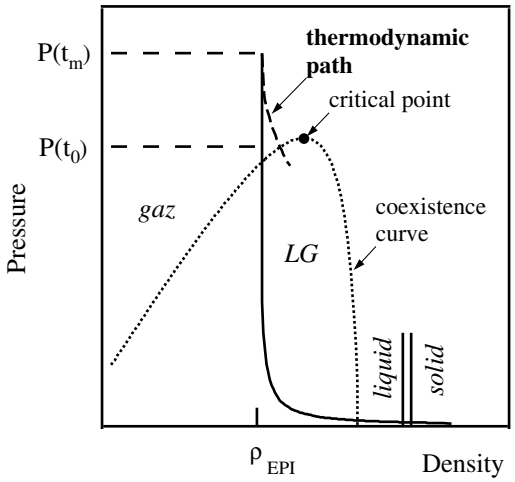

FIG. 1. Schematic representation of the thermodynamic path in the vessel in a density-pressure plane (the dashed line shows the TP during cooling). The sample goes from the solid-state at normal density and room temperature to a well-known average density plasma, through a two-phase liquid-gas region (noted *LG*), in which the increase of pressure before isochoric heating is due to the residual atmosphere initially present in the vessel.

conductivity and pressure at time t_m. Cooling begins beyond this point. During cooling, the plasma is polluted by the wall ablation, as experimentally observed and shown in Fig. 2, where the TP's during heating and cooling deviate from each other at time t_1. Because of the wall ablated mass introduced in the vessel after t_1, TP is unknown and is therefore partially drawn in the Fig. 1 (dashed line). Finally, the interpretation of the measured data in terms of state variables is meaningful only at times when the plasma is homogeneous and not yet polluted by the wall ablation, i.e., between t_0 and t_1. At each shot, the input electrical energy is inferred from the current and voltage measurements with a 15% uncertainty. ΔU_{int} can be evaluated from the input energy. As the thermal losses are assumed to be radiative, the internal energy is obtained at each time by solving a differential equation which depends on the electrical energy and the temperature T of the plasma [4]. T has been written as a function of U_{int} by using SESAME tables. We have checked that changing the relationship between T and U_{int} using a simple linear rule instead of SESAME have a negligible impact on the results (i.e., few percent).

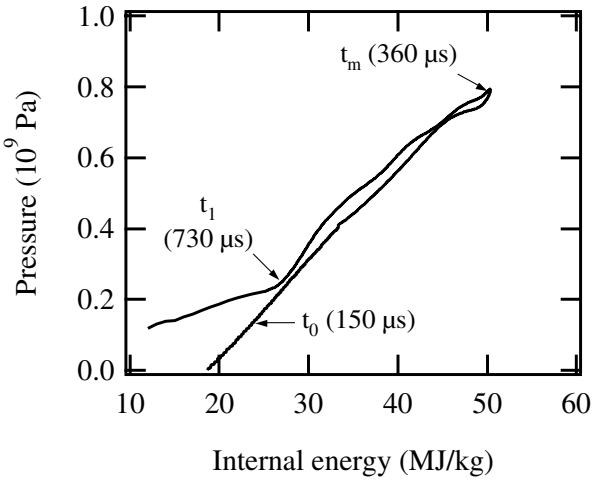

FIG. 2. Measured thermodynamic path of aluminum in a pressure-internal energy plane (nominal density 0.1 g/cm^3).

We present five EOS models of aluminum dense plasmas: the quotidian equation of state (QEOS) model [5], the SESAME (S3718) tables [2], the Bushman, Lomonosov, and Fortov (BLF) model [6], the molecular dynamic (MD) Vienna *ab initio* Simulation Program (VASP) [7], and SCAALP, an average atom model based on the density functional theory (DFT) for hot dense plasmas [4].

In QEOS, thermodynamic functions of electrons and ions are calculated separately. Electronic properties are obtained from a modified Thomas-Fermi statistical model, and the ionic part is described by a Debye model for the solid phase and an interpolation between the Dulong-Petit solid at the melting temperature and the perfect gas at high-temperature for the fluid phase. Because the largest inaccuracy in the Thomas-Fermi pressure P occurs near the cold solid, the electronic part is corrected by an empirical volume-dependent bounding term which enforces the conditions $P = 0$ at the reference density and temperature.

The SESAME library has been constructed with different theoretical models. In the thermodynamic range of EPI data, SESAME is an interpolation between the results of several theories valid in adjacent domains: a soft-sphere liquid domain at low-temperature below the saturation curve, a Saha model for temperature below approximately 3 eV, and then an activity expansion model (ACTEX), based on screened potentials, at higher temperature.

The BLF model is a wide-range EOS of metals which allows one to calculate thermodynamic properties of metals in solid, liquid, and plasma states as well as in two-phase solid-liquid and liquid-gas regions. The electronic contribution takes into account degenerated electron gas, effects of metal-insulator transition, and single Saha ionization. The model describes the disordered electron system and the partially ionized plasma formed near the liquid-vapor equilibrium curve and the critical point.

In VASP, the energetics of the system and the forces on the ions are calculated by first principles methods, leading to an ionic structure consistent with the degeneracy of the electrons. VASP calculations are performed in the framework of DFT, at the level of generalized gradient approximation for exchange and correlation energies [8]. Vanderbilt ultrasoft pseudopotentials [9] or projector augmented wave potentials [10] have been used to describe the electron-ion interactions, leading to similar values of

pressure and internal energy. Pressures were averaged on 32 particles (0.3 g/cm^3) and 16 particles (0.1 g/cm^3) MD simulations of 300–500 time steps after equilibration. Calculations have been done at Γ point, and convergence in k vectors checked on some specific configurations.

In SCAALP, electronic structure and ionic distribution are determined self-consistently. The model takes into account the polarization and the correlation effect of the continuum electrons, as well as a part of the exchange interaction within the interatomic effective potential, and gives access to the excess free energy of the ionic subsystem. The exchange and correlation functional is the same as in VASP, leading to a version called SCAALP-0T. Additional calculations include a finite-temperature exchange and correlation correction [11]; this version is noted SCAALP-FT. We look for the best reference system using the Gibbs-Bogolyubov inequality [12] to get the radial distribution function of the ionic subsystem from the interatomic effective potential. One-component plasma and hard sphere were used as reference systems, leading to similar values of calculated pressure and mean ionization. All the presented results are obtained with the hard sphere as reference system. The calculated internal reference energy of the cold solid aluminum is -483.4225 and -485.7087 Ryd for SCAALP-0T and SCAALP-FT, respectively. Pressure and internal energy are obtained by numerical differentiation of free energy.

Experimental pressure of aluminum as a function of internal energy variation is plotted in Fig. 3 for a density of 0.1 g/cm^3 and in Fig. 4 for a density of 0.3 g/cm^3. Results from the five EOS models are also shown. Theoretical reference energy is the internal energy at solid density and room temperature. We can see that most of the calculated pressures are higher than the experimental measurements. VASP, QEOS, and SESAME results are quite similar and the best agreement with the measured isochores is obtained with BLF. QEOS is known to produce accurate results in various case (normal solid conditions, high-density and/or high-temperature limit, and low-density limit) while in the more complicated region of low-temperature expanded states, i.e., EPI range, its accuracy does not match that of BLF or experimental results. The critical point of aluminum calculated with QEOS is located at $\sim$0.76 g/cm^3 and $\sim$12 100 K. However, isobaric expansion measurements performed by Gathers and Ross [13] have been analyzed with the soft-sphere model developed by Young [14] to yield a critical temperature of 5726 K [note that the BLF critical temperature is equal to $\sim$6400 K]. Therefore, in the EPI range, we confirm that QEOS is not very accurate [15].

A disagreement between VASP and EPI data is observed. Here, in the regime of partially ionized plasmas, the EOS predictions obtained from quantum MD codes are as accurate as the results from the interpolated SESAME tables. We can see in the figures that the agreement is better for the 0.3 g/cm^3 case (Fig. 4) than for the 0.1 g/cm^3 case (Fig. 3), showing that VASP accuracy improves when aluminum density increases. SCAALP results agree well with experimental values at 0.1 g/cm^3. Theoretical pressures from SCAALP-0T and SCAALP-FT are similar, showing that the influence of exchange-correlation treatment has a minor impact on theoretical results in this particular regime. At 0.3 g/cm^3, SCAALP results overestimate the internal energy variation and are not presented. The disagreement at this density might be due to the treatment of density effects. Indeed, SCAALP calculations indicate that the $3p$ orbital is not bound in the internal energy range considered. Then, the statistical contribution of neutral species, which are known to be important in this thermodynamic range [16,17], cannot be taken into account in the mean-field calculations, leading to an overestimation of internal energy variation.

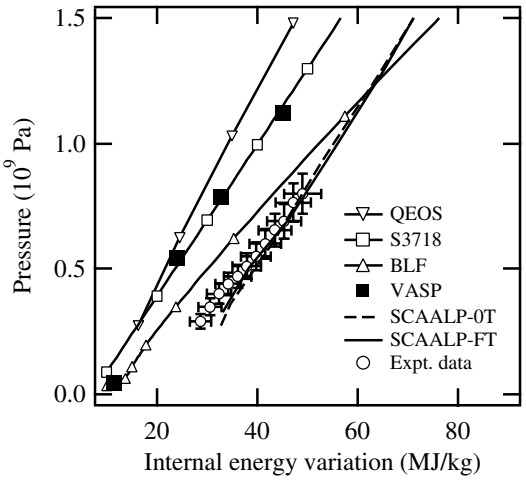

FIG. 3. Pressure of aluminum at a density of 0.1 g/cm^3 as a function of internal energy variation. Theoretical results from the five EOS models are also shown.

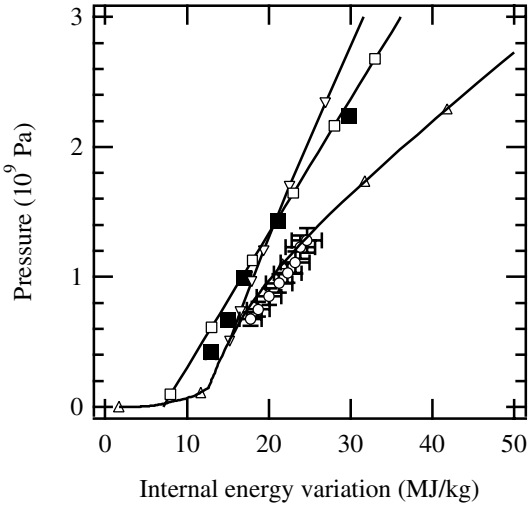

FIG. 4. Same as Fig. 3 for aluminum at a density of 0.3 g/cm^3.

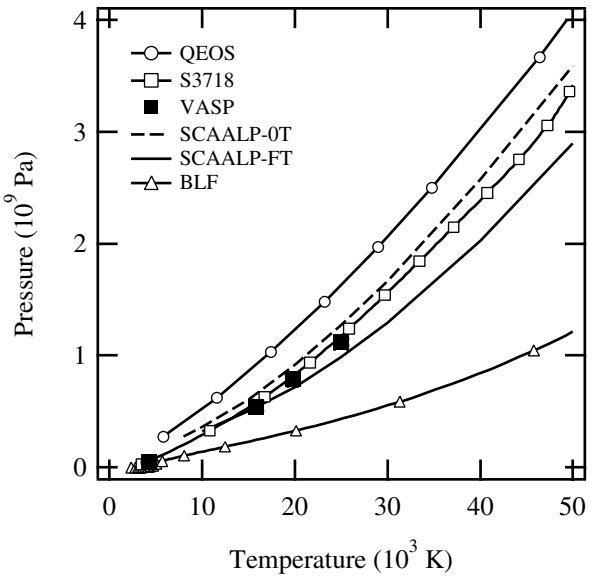

FIG. 5. Pressure of aluminum at a density of 0.1 g/cm^3 as a function of temperature, calculated in the five theoretical models.

At 0.1 g/cm^3 and temperature lower than 40 000 K, 80% to 90% of the pressure calculated by SCAALP is due to the ionic contribution P_{ion}. P_{ion} from QEOS, from SCAALP, and total pressure calculated by VASP are very close. Then, the difference between the models mentioned above can be attributed to the treatment of the electronic contribution to the EOS in the regime shown in Fig. 3.

A direct code-to-code comparison is shown in Fig. 5. Pressures from the five EOS models are shown as a function of temperature, in the case of aluminum at a density of 0.1 g/cm^3. Again, a dispersion between theoretical data is observed. Note that the BLF pressure is 4 times lower than the QEOS pressure at 40 000 K. SESAME, SCAALP, and VASP are very close. A weak but non-negligible effect of the exchange-correlation treatment is noticed: SCAALP-FT pressure is smaller than SCAALP-0T pressure. Temperature measurements would be necessary to distinguish such effect.

To summarize, we have carried out an experiment measuring pressure, mass density, and internal energy variation of an aluminum plasma in the density and internal energy range (0.1–0.3 g/cm^3; 20–50 MJ/kg), allowing an unequivocal test of the validity of different equation of state models in warm dense matter. In the studied thermodynamic regime, experimental pressures are in good agreement with the BLF model, showing that an accurate description of the SCP formed in the vicinity of the liquid-vapor equilibrium curve has a strong impact on theoretical results. SCAALP results are in good agreement with experimental isochores at 0.1 g/cm^3. A small but non-negligible influence of exchange-correlation treatment is emphasized by the model. A comparison between experimental and VASP isochores shows that VASP accuracy improves with increasing density. These results should be a challenge for performing accurate experiments and validating theoretical models in warm dense matter.

It is a pleasure to thank B. Loffredo and M. Sonnaert for their technical assistance during the course of this work. We also thank P. Combis for making the results of the BLF code available and M. P. Desjarlais for useful discussions.

*Electronic address: patrick.renaudin@cea.fr

[1] S. Ichimaru, *Statistical Plasma Physics: Condensed Plasmas* (Addison-Wesley, New-York, 1994), Vol. II.
[2] S. P. Lyon and J. D. Johnson, *T-1 Handbook of the SESAME Equation of State Library*, Vol. 1, p. 3718, Report No. LA-CP-98-100.
[3] F. Perrot, M. W. C. Dharma-Wardana, and J. Benage, Phys. Rev. E **65**, 46414 (2002).
[4] P. Renaudin, C. Blancard, G. Faussurier, and P. Noiret, Phys. Rev. Lett. **88**, 215001 (2002).
[5] R. M. More, K. H. Warren, D. A. Young, and G. B. Zimmerman, Phys. Fluids (1958–1988) **31**, 3059 (1988).
[6] A. V. Bushman, I. V. Lomonosov, and V. E. Fortov, *Equations of State of Metals at High Energy Densities* (Institute of Chemical Physics, Russian Academy of Sciences, Chernogolovka, 1992) (in Russian).
[7] G. Kresse and J. Hafner, Phys. Rev. B **47**, 558 (1993).
[8] Y. Wang and J. P. Perdew, Phys. Rev. B **44**, 13 298 (1991).
[9] D. Vanderbilt, Phys. Rev. B **41**, 7892 (1990).
[10] G. Kresse and D. Joubert, Phys. Rev. B **59**, 1758 (1999).
[11] H. Iyetomi and S. Ichimaru, Phys. Rev. A **34**, 433 (1986).
[12] R. P. Feynman, *Statistical Mechanics: A Set of Lectures* (Addison-Wesley, New-York, 1972).
[13] G. R. Gathers, Int. J. Thermophys. **4**, 209 (1983); G. R. Gathers and M. Ross, J. Non-Cryst. Solids **61–62**, 59 (1984).
[14] D. A. Young, Lawrence Livermore National Laboratory, Report No. UCRL-52352, 1977 (unpublished).
[15] An improved version of QEOS with a more accurate description of the liquid-vapor equilibrium can be found in P. Celliers and A. Ng, Phys. Rev. E **47**, 3547 (1993); D. A. Young and E. M. Corey, J. Appl. Phys. **78**, 3748 (1995).
[16] F. Perrot and M. W. C. Dharma-wardana, Phys. Rev. E **52**, 5352 (1995).
[17] R. Redmer, Phys. Rev. E **59**, 1073 (1999).